# COMPARISON OF MODELLING APPROACHES FOR CFD SIMULATIONS OF HIGH PRESSURE HYDROGEN RELEASES

**Papanikolaou, E.[1] and Baraldi D.[1]**
**[1] European Commission DG-JRC, Institute for Energy, P.O. Box 2, 1755 ZG, Petten, The Netherlands.**
**Efthymia.PAPANIKOLAOU@ec.europa.eu**
**daniele.baraldi@jrc.nl**

**ABSTRACT**

Several approaches have been used in the past to model the source of a high pressure under-expanded jet such as the computationally expensive resolution of the jet shock structure and the simpler pseudo-source or notional nozzle approaches. In each approach assumptions are made introducing inaccuracies in the CFD calculations. This work assesses the effect of different source modeling approaches on the accuracy of CFD calculations by comparing simulation results to experimental data of the axial distribution of the flow velocity and $H_2$ concentration.

## 1.0 INTRODUCTION

Gaseous $H_2$ will be stored and distributed at high pressures to increase the energy density and transport capacity of the system. The accidental release from high pressure systems may lead to a jet of several meters size. The jet will be under-expanded close to the release point and will rapidly accelerate and expand to atmospheric pressure through a series of shocks. The numerical modeling of the shock region is quite demanding in order to have a satisfactory grid resolution. Together with the need for a long enough computational domain to encompass the jet at its full extent, the numerical effort can be extremely intensive. For example, Xu et al. (2005) [1] used a mesh of 200.000 nodes to model only ¼ of the shock region of a $H_2$ release from a 20 MPa vessel through a nozzle of 1 mm. Also, Cumber et al. (1995) as cited in the Final Modelling Report, HYPER (2008) [2], considered a grid resolution between 1/32 to1/64 of the actual diameter to ensure grid independence. To bypass such demands, several approaches replacing the actual nozzle by a notional nozzle (often referred to as fictitious or pseudo-diameter) occupying an area with the same flow rate as the real one and at ambient pressure and uniform sonic velocity have been proposed in the past. These approaches have been implemented in several numerical investigations. For example, Venetsanos et al. (2010) [3] used the Birch 1984 [4] approach to model horizontal $H_2$ releases of several experiments such as a release from a 3 mm diameter nozzle with 10 MPa stagnation pressure, a release from a 0.25 mm diameter nozzle with 16 MPa stagnation pressure and releases from 0.8, 1.6 and 8 mm diameter nozzles at 40 MPa. The authors reported a good agreement with the experimental measurements. In the Standard Benchmark Problem [5] of a $H_2$ release and dispersion from $CGH_2$ bus in an underpass the majority of the participants used notional nozzle approaches to model the 35 MPa pressure $H_2$ release. Venetsanos et al. (2008) [6] used a notional approach to model several $H_2$ and $CH_4$ releases from compressed gaseous systems at 20, 35 and 70 MPa. Ivings et al. (2010) [7] used also a notional nozzle approach to model the release of $CH_4$ with pressures ranging from 0.85 to 10 barg inside a mechanically ventilated room and reported good predictions. Brennan et al. (2009) [8] presented a Large Eddy Simulation (LES) approach to model high pressure jet fires and compared their results against a large scale vertical $H_2$ jet fire test. They used a notional nozzle approach derived from the conservation of mass and energy assuming non-ideal gas properties. Hourri et al. (2009) [9] compared the numerical results of the LFL extent of vertical free $H_2$ and $CH_4$ jets to the predictions of the Birch 1984 [4] and Schefer 2007 [10] which use the respective notional nozzle approaches and found good agreement. Tchouvelev (2008) [11] presented a comparison between the results of the actual and a notional nozzle approach (similar to Birch 1984) of a $H_2$ release at 430 bars and found that the notional approach produced 25-30% longer extents of the flammable cloud. The author attributed the difference to the use of real gas properties in the actual leak modeling in contrast to the ideal properties in the notional

approach and the different input sound velocity of the jet. The validation of the notional nozzle approaches have been recently identified by Baraldi et al. (2010) [12] as an issue that needs to be investigated. This issue has also been suggested for further investigations earlier by the HySafe consortium [13].

This work assesses the effect of different source modeling approaches on the accuracy of the CFD calculations by comparing simulation results to experimental data of the axial distribution of the flow velocity and $H_2$ concentration of an under-expanded jet.

## 2.0 NOTIONAL NOZZLE APPROACHES

This paragraph describes in detail the most widely used approaches: the Birch 1984 [4], the Birch 1987 [14], the Ewan and Moodie (1986) [15] and the Schefer (2007) [10]. These approaches are assessed by comparing the simulation results to experimental data of the axial velocity and $H_2$ concentration of a high pressure horizontal jet. Apart from the approaches presented here, approaches that take into account also the conservation of energy have been proposed, such as the one by Xiao et al. (2005) [16] assuming real gas properties and by Yüceil and Ötügen (2002) [17] assuming ideal gas properties. It is interesting to note that the approach by Xiao et al. (2005) [16] predicts at the notional nozzle a temperature far less than the stagnation one. Also, Molkov et al. (2009) [18] as cited in [12] proposed an approach to calculate the notional nozzle diameter assuming the conservation of mass and energy together with the Abel-Noble equation for the calculation of the gas properties.

### 2.1 Birch 1984 approach

Birch, et al. (1984) [4] studied experimentally the concentration field in compressible sonic jets of natural gas over the pressure range from 2 to 70 bar using gas chromatography. They introduced a "pseudo-diameter" which when substituted into the equations defining a subsonic round free jet, will reproduce the concentration field in the self-preserving region of the supercritical jet release. The mass flow rate through the area of the "pseudo-diameter" was considered to be equal to the one through the real orifice but at ambient temperature and pressure and with uniform sonic velocity.

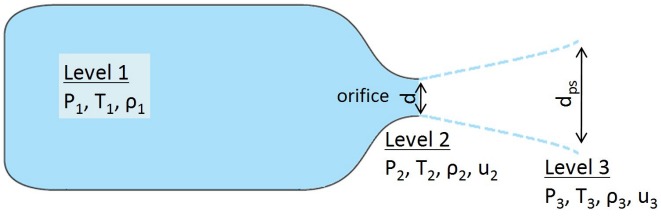


Figure 1. Under-expanded gas release from an infinite reservoir (level 1) through an orifice of diameter d (level 2) showing also the expansion to ambient conditions at the notional location (level 3)

It is worth to note that level 3 in Figure 1 does not necessarily exist in the physical sense but was postulated to agree with the chosen definition of the "pseudo-diameter".

For 1D compressible flow, the mass conservation of the expansion area (area between level 2 and 3) takes the following form:

$$\dot{m} = C_d \rho_2 u_2 A_2 = \rho_3 u_3 A_3 \quad (1)$$

where $C_d$ is the discharge coefficient at level 2 (non uniform velocity profile at this level), $u_2$ the local sonic velocity, $A_2$ the area of the orifice, $A_3$ the notional area, $\rho_2$ and $\rho_3$ the density of the jet

at level 2 and 3 and $u_3$ the sonic velocity at ambient conditions. At level 3, no discharge coefficient is required since the profile is assumed uniform in the definition of the "pseudo-diameter".

From Eq. (1) the calculation of the "pseudo-diameter" is given by:

$$\frac{d_{ps}^2}{d^2} = \frac{C_d \rho_2 u_2}{\rho_3 u_3} \tag{2}$$

Assuming isentropic change between level 1 and 2, the temperature $T_2$ and pressure $P_2$ at level 2 are calculated by:

$$T_2 = T_1\left(\frac{2}{\gamma+1}\right) \tag{3}$$

$$P_2 = P_1\left(\frac{2}{\gamma+1}\right)^{\frac{\gamma}{(\gamma-1)}} \tag{4}$$

where $\gamma(=1.41)$ is the ratio of the heat capacity at constant pressure to the heat capacity at constant volume.

Assuming ideal gas, the density at level 2 is calculated by:

$$\rho_2 = \frac{P_1\left(\frac{2}{\gamma+1}\right)^{\frac{1}{(\gamma-1)}} MW}{RT_1} \tag{5}$$

where $MW$ is the molecular weight of the released gas and R the universal gas constant.

The sonic velocity at level 2 is proportional to the square root of the local temperature $T_2$ and in turn to the square root of the stagnant temperature $T_1$:

$$u_2 = \sqrt{\frac{\gamma R T_2}{MW}} = \sqrt{\frac{\gamma R T_1\left(\frac{2}{\gamma+1}\right)}{MW}} \tag{6}$$

Similarly, at level 3 the sonic velocity $u_3$ is given by:

$$u_3 = \sqrt{\frac{\gamma R T_3}{MW}} \tag{7}$$

And density by:

$$\rho_3 = \frac{P_3 MW}{RT_3} \tag{8}$$

Substituting equations (5), (6), (8) and (7) into equation (2):

$$\frac{d_{ps}^2}{d^2} = C_d \frac{P_1}{P_3}\left(\frac{2}{\gamma+1}\right)^{\gamma+1/2(\gamma-1)} \sqrt{\frac{T_3}{T_1}} \tag{9}$$

Finally, by assuming that the upstream temperature is approximately ambient ($T_1 \approx T_3$) equation (9) is reduced to:

$$\frac{d_{ps}^2}{d^2} = C_d \frac{P_1}{P_3}\left(\frac{2}{\gamma+1}\right)^{\gamma+1/2(\gamma-1)} \tag{10}$$

### 2.2 Birch 1987 approach

Birch et al. (1987) [14] proposed an improved "pseudo-diameter" definition based not only on the conservation of mass as in their former definition (Birch et al., 1984) but also in the conservation of momentum through the expansion area. The assumption that the pressure at level 3 is reduced to ambient is retained.

Conservation of momentum:

$$\rho_3 u_3^2 A_3 = C_d^2 \rho_2 u_2^2 A_2 + A_2\left(P_2 - P_3\right) \tag{11}$$

From equations (11), (5), (6) and (1), the velocity at level 3 is given by:

$$u_3 = u_2\left(C_d + \frac{1 - \frac{P_3}{P_1}\left(\frac{2}{\gamma+1}\right)^{-\gamma/(\gamma-1)}}{\gamma C_d}\right) \tag{12}$$

For high pressures at the reservoir (where $\frac{P_1}{P_3} >> \left(\frac{2}{\gamma+1}\right)^{-\gamma/(\gamma-1)}$) equation (12) is simplified to:

$$u_3 \approx u_2\left(C_d + \frac{1}{\gamma C_d}\right) \tag{13}$$

Finally, the "pseudo-diameter" is given by:

$$d_{ps} = d\sqrt{\frac{u_2}{u_3} C_d \frac{P_1}{P_3}\left(\frac{2}{\gamma+1}\right)^{1/(\gamma-1)}} \tag{14}$$

### 2.3 Ewan and Moodie approach

Similarly to the Birch 1984 [4] approach, Ewan and Moodie (1986) [15] used the mass conservation equation and suggested that the jet at level 3 is sonic, at atmospheric pressure and with the same mass flow rate as in level 2. However, based on experimental data of under-expanded air jets at pressures up to 20 bars, they proposed that the jet at level 3 should have a temperature equal to the one at level 2 (instead of being equal to the atmospheric as in the previous Birch approaches), i.e. $T_3 = T_2$. The equations for the calculation of the "pseudo-diameter" and velocity at level 3 are:

$$d_{ps} = d\sqrt{C_d \frac{P_2}{P_3}} \tag{15}$$

$$u_3 = \sqrt{R_g \gamma T_3} \tag{16}$$

### 2.4 Schefer approach

Schefer et al. (2007) [10] proposed an approach analogous to Birch et al. (1987) [14] using both the conservation of mass and momentum, assuming no viscous losses and again a uniform profile across the "pseudo-diameter" cross section. For the calculation of isentropic relations to $H_2$ tank blow down and for pressures higher than 170 bars Schefer et al. (2007) [10] proposed the use of the Abel-Nobel equation of state:

$$P = \frac{\rho R_{H_2} T}{(1 - b\rho)},\ b = 7.691 \times 10^{-3}\, m^3/kg \text{ and } R_{H_2} = 4124\ N\ m/kg\ K \tag{17}$$

Equation (17) is used to calculate the stagnation density: $\rho_1 = \frac{P_1}{P_1 b + R_{H_2} T_1}$

Furthermore, assuming isentropic expansion and sonic flow at level 2, the density is given by:

$$\left(\frac{\rho_1}{1 - b\rho_1}\right)^{\gamma} = \left(\frac{\rho_2}{1 - b\rho_2}\right)^{\gamma} \left[1 + \left(\frac{\gamma - 1}{2(1 - b\rho_2)^2}\right)\right]^{\gamma/(\gamma - 1)} \tag{18}$$

Furthermore, the temperature, pressure and sonic velocity at level 2 are given by:

$$T_2 = \frac{T_1}{1 + \frac{\gamma - 1}{2(1 - b\rho_2)^2}} \tag{19}$$

$$P_2 = \frac{\rho_2 R T_2}{1 - b\rho_2} \tag{20}$$

$$u_2 = \frac{1}{(1 - b\rho_2)} \sqrt{\gamma R T_2} \tag{21}$$

## 3.0 EXPERIMENTAL DESCRIPTION

The experiments covered horizontal high momentum $H_2$ releases in the HYKA test site of the Institute for Nuclear and Energy Technologies of the FZK. They were designed to evaluate the flammable $H_2$/air mixture in free turbulent jets at different pressures. The jet was released from a bulk vessel at different initial pressures and from different nozzle diameters ranging from 0.16 mm to 1 mm. The dimensions of the test site were 5.5 m by 8.5 m by 3.4 m and the release orifice was located 0.9 m above the ground to avoid wall effects. Hydrogen concentration and flow velocity were measured at either three or two different cross-sections at distances 0.75 m, 1.5 m and 2.25 m from the nozzle. For more details on the experiments the reader is referred to [19] and [20]. From the set of experiments, the test with an initial $H_2$ pressure of 98.1 bars at temperature of 14.5 ºC issuing from a 1 mm diameter nozzle was selected for the assessment of the notional nozzle approaches.

## 4.0 SIMULATIONS SET UP

The Table 1 presents the release conditions as calculated from each of the approaches. The velocity at the notional nozzle from Birch 1984 and Ewan and Moodie is sonic, whereas the one from Birch 1987 and Schefer is higher. The latter two approaches take into account the momentum conservation thereby it is assumed that all of the excess pressure (the difference between the pressure at the real nozzle and the atmospheric) goes to increasing the jet's momentum. A discharge coefficient $C_d$ equal to 0.91 was chosen to match the calculated mass flow-rate of the simulations to the experimental one.

Table 1. Conditions at level 3 (pseudo-diameter $d_{ps}$ location) based on the different approaches and conditions at level 2 assuming either real or ideal gas properties

| Conditions at level 3 (pseudo-diameter location) | | | | | |
|---|---|---|---|---|---|
| Approach | $d_{ps}$ (m) | source area ($m^2$) | $\rho_3$ ($kg/m^3$) | $T_3$ (K) | $u_3$ (m/s) |
| Birch 1984 | $7.14 \cdot 10^{-3}$ | $4 \cdot 10^{-5}$ | 0.0854 | 288 | 1293 |
| Birch 1987 | $5.78 \cdot 10^{-3}$ | $2.62 \cdot 10^{-5}$ | 0.0854 | 288 | 1972 |
| Ewan and Moodie | $6.81 \cdot 10^{-3}$ | $3.64 \cdot 10^{-5}$ | 0.1029 | 239 | 1178 |
| Schefer | $5.86 \cdot 10^{-3}$ | $2.69 \cdot 10^{-5}$ | 0.0854 | 288 | 2029 |
| Conditions at the nozzle – level 2 (assuming isentropic expansion) | | | | | |
| | $P_2$ (kPa) | $\rho_2$ ($kg/m^3$) | | $T_2$ (K) | $u_2$ (m/s) |
| Ideal gas | 5165 | 5.2469 | | 239 | 1178 |
| Real gas (Abel-Nobel) | 4932 | 4.8867 | | 235 | 1216 |

The dispersion predictions resulting from the release conditions of each approach were assessed in connection to four commonly used turbulence models: the standard k-$\varepsilon$ epsilon, the Shear Stress Transport (SST), the ReNormalization Group (RNG) k-$\varepsilon$ and the Baseline k-omega (BSL) [21]. For comparison reasons, it was decided to simulate the $H_2$ release from a pipe of 10D length having a diameter equal to the experimental. This case will be referred to as "pipe" as from now.

The numerical calculations were performed with ANSYS-CFX version 12.1 [22]. The following set up was applied for the simulations:

- All simulations were considered as transient physical processes.
- The multi-component fluid consisted of $O_2$, $N_2$ and $H_2$.
- The High Resolution scheme of CFX was used for the discretization of the advection terms. The scheme has a blending factor which allows to be switched to the First Order Advection scheme based on the local variable gradients.
- The Second Order Backward Euler discretization scheme was used for the transient terms.
- The total energy option was selected. This option models the transport of enthalpy including kinetic energy effects which become significant in gas flows where the Mach number exceeds 0.3.
- The ideal gas law was applied to the simulations with release conditions calculated from the notional nozzle approaches. For the "pipe" cases, $H_2$ was treated as a real gas. Three equations of state are available as built-in options in CFX, with the standard Redlich Kwong being the

default and the chosen one for simulating $H_2$ as a real gas. The rest of the components were treated as ideal gases.

- Stagnant conditions were assumed as the initial state with atmospheric pressure and temperature equal to 14.5 ºC.

- The velocity and temperature, as calculated from the notional nozzle approaches, were specified at the inlet. On the other hand, a mass flow rate equal to 4.42 g/s was assumed for the "pipe" cases based on the $H_2$ stagnant conditions of the experiment. All simulations had a common incoming level of turbulence (intensity equal to 5%) assigned to the inlet for the calculation of the turbulent quantities k and $\varepsilon$. The importance of the level of turbulence has been investigated by Brennan et al. (2009) [8]. The authors concluded that for moderate grid resolution, the turbulence intensity has a weak effect on the predictions, provided that its value is less than 30%.

- The dimensions of the computational domain were 15 m by 10 m by 10 m. The ground was defined as wall (no slip boundary condition), the west (W) and top planes as openings (relative total pressure for inflow and relative static pressure for outflow set to zero, zero gradient for k and $\varepsilon$), the east (E) plane as an outlet (averaged relative static pressure set to zero) and finally for the north (N) and south (S) planes a symmetry assumption (zero normal velocity component and zero normal scalar variable gradients) was made (see Figure 2).

- CFX presents the normalized residuals to judge convergence. The maximum allowed RMS normalized residual was set to $5\times10^{-4}$ with a maximum number of coefficient iterations equal to 8 for the notional nozzle simulations and between 10 and 20 for the "pipe" cases.

- For the simulations using the notional nozzle approaches, the initial time step was $5\times10^{-7}$ s and the minimum and maximum was $10^{-8}$ s and $10^{-3}$ s respectively. The time step size was automatically adapted according to the number of the minimum and maximum coefficient loops which were set to 3 and 6 respectively. If the actual number of coefficient loops used is less than the minimum assigned number, the timestep size is increased. The opposite holds for the decrease of the timestep size based on the maximum value of the coefficient loops.

- For the simulations of the "pipe" cases, the initial time step was $10^{-8}$ s and the minimum and maximum was $10^{-8}$ s and $10^{-4}$ s respectively. The minimum and maximum coefficient loops were kept the same as in the previous set of simulations.

- The mesh used was unstructured. The first set of simulations was the one of the Birch 1987 approach. A mesh of approximately 50.000 nodes was used with a minimum resolution of $8\times10^{-4}$ m at the source. The resolution at the measurement points of 1.5 m and 2.25 m was in the range of 0.14 m to 0.18 m. The resolution of the mesh was such that the anticipated solution would be obtained in a reasonable for engineering applications time. Indeed, for 5 s of simulation time, the wall clock time was between 5 to 6 h. This set of simulations will be referred to as "coarse" as from now. For the same approach, a finer mesh was used to test the sensitivity of the predictions. The mesh consisted of approximately 250.000 nodes with a minimum resolution of $3\times10^{-4}$ m at the release. The resolution at the 2 measurement points was in the range of 0.06 m to 0.11 m. The simulations had an average wall clock time of 30 h. As it will be shown in the following paragraphs, the results with the finer mesh showed generally a tendency to over-predict the $H_2$ concentration by 3% to 17% and the velocity by 7% to 21%. Based on the findings of the first set of simulations it was decided to keep the fine mesh for the rest of the notional nozzle approaches. The simulations with the fine mesh will be referred to as "fine" as from now. For the sake of comparison, the simulations of the "pipe" cases were at first done with a mesh that would give a solution at a wall clock time between the previously investigated "coarse" and "fine" cases. The mesh was around 65.000 nodes and the wall clock time was between 15 to 18 h. Again, to test the sensitivity of the predictions to

the mesh, a finer by roughly 2 times mesh was used. The wall clock time of the simulations was between 8 to 9 days. Both the fine and the coarse mesh of the "pipe" cases had a resolution at the nozzle of $6.5\times10^{-5}$ m (this size order was kept for a volume close to the pipe outlet and as far from it as approximately 10 pipe diameters) whereas at the 2 measurement points it ranged from 0.12 m to 0.14 m at 1.5 m and 0.02 m to 0.04 m at 2.25 m.

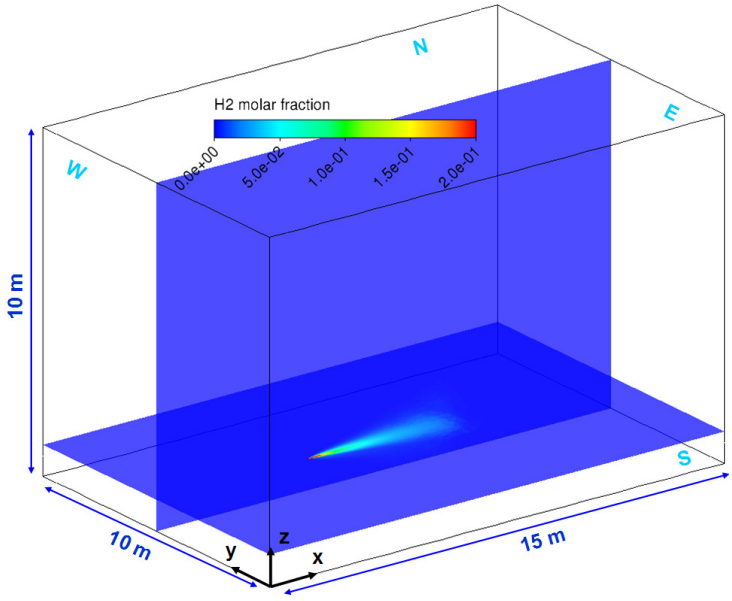


Figure 2. Domain size used for all simulations

## 5.0 SIMULATIONS RESULTS

Figures 3 and 4 show the numerical predictions of the $H_2$ volumetric concentration and velocity at 1.5 m and 2.25 m from the release point in comparison to the experimental data. For each figure, the blue horizontal line shows the Mean Experimental Value (MEV). The two dotted blue lines are the MEV minus/plus the Standard Deviation (STD) of the experimental data. In order to have a convenient and general quantitative assessment of the numerical predictions, each figure has two sets of horizontal lines, the black represent a 30% over/under prediction of the MEV and the grey show the 50% over/under prediction of the MEV. The graphs are divided into 5 columns, each one of them for each modeling approach (i.e. actual pipe and notional nozzle approaches). The predictions of the "coarse" cases are given in square markers and the "fine" in diamond. Finally, each colour is assigned to a turbulent model (i.e. grey for k-$\varepsilon$, red for SST, blue for RNG and green for BSL).

By comparing the predictions of the $H_2$ % concentration by volume (Figure 3 and Figure 4) the following general conclusions can be drawn:

- The Birch 1987 and Schefer approaches seem to perform better than the Birch 1984 and Ewan. It is interesting to note that the momentum flux at the source was higher for the Birch 1987 and Schefer approaches (8.72 and 9.47 kg m $s^{-2}$ respectively) as compared to the Birch 1984 and Ewan (5.71 and 5.21 kg m $s^{-}2$ respectively). Apparently, the initial momentum flux affects considerably the spreading rate of $H_2$ concentration along the centreline.

- By comparing the different turbulent models, approach by approach, it seems that there is a general tendency for higher predictions with k-$\varepsilon$, followed by RNG, BSL and finally SST. For all notional nozzle approaches, the predictions at 1.5 m with k-$\varepsilon$ were higher than the 30% of MEV and in half of them the predictions were as high as almost 100% of the MEV.

For the Birch 1987 and Schefer, the predictions from the rest of the turbulent models lie in the area bounded by the MEV +/- STD.

- For the "pipe" cases, it seems that the coarse mesh predicted the concentrations satisfactorily. All predictions, including the ones with the finer mesh, were within the area of 30% MEV over/under-prediction.

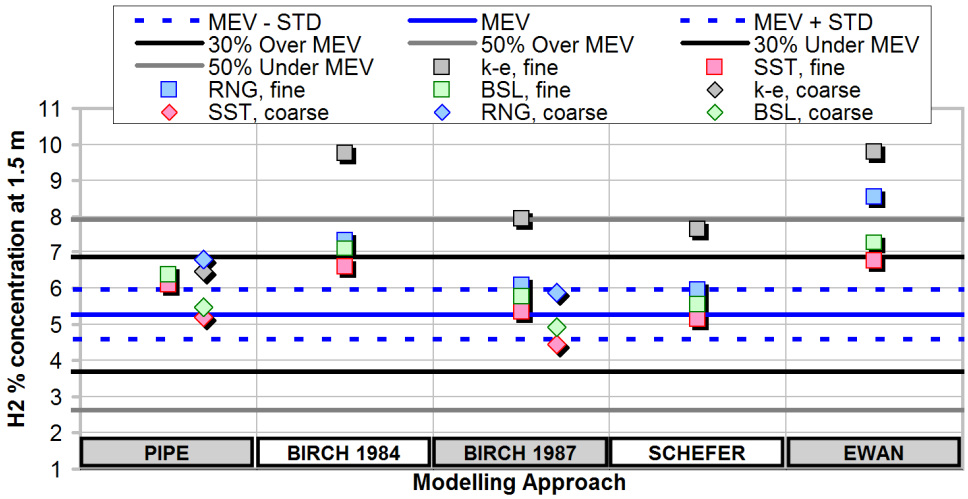


Figure 3. $H_2$ % volumetric concentration at 1.5 m from the release at the jet's centerline for all simulations considered

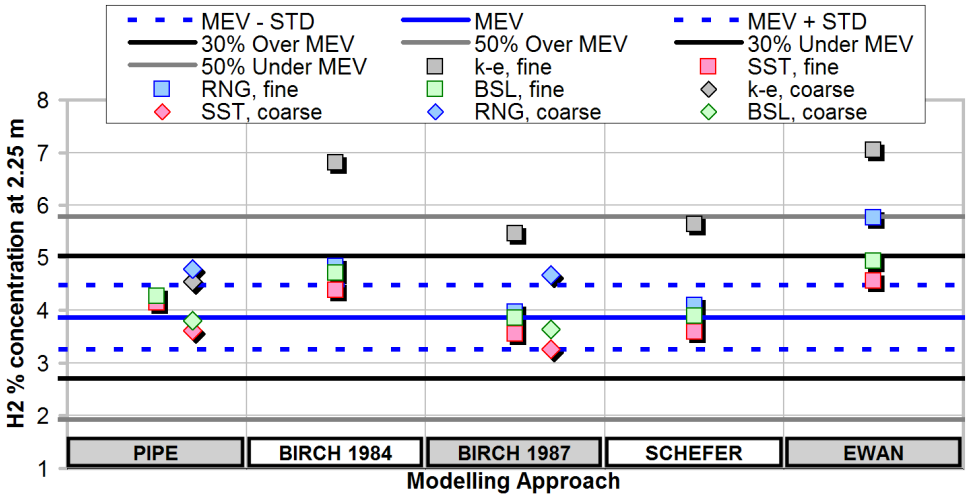


Figure 4. $H_2$ % volumetric concentration at 2.25 m from the release at the jet's centerline for all simulations considered

By comparing the predictions of the velocity (Figure 5 and Figure 6) at 1.5 m and 2.25 m from the release at the jet's centerline, the following general conclusions can be drawn:

- The majority of the predictions were located within the 30% MEV over/under-prediction lines.

- As expected, the highest values were predicted by the approaches that had the highest release velocity, i.e. the Schefer approach with 2029 m/s release velocity and the Birch 1987 approach

with 1972 m/s release velocity (see Table 1). The lowest values were predicted by the Ewan approach which had the lowest release velocity (1178 m/s).

- By comparing the different turbulent models, approach by approach, it seems that again there is a general tendency for higher predictions with k-$\varepsilon$, following by either RNG or BSL and lastly SST. The k-$\varepsilon$ model is known to give poor predictions of the mean velocity profiles of turbulent axisymmetric jets. Furthermore, as the jet velocity increases, the model prediction deviates increasingly from the experimental measurements [23]. As mentioned by Wilcox [24], the velocity spreading rate, predicted by k-e, may be 25% to 40% higher than the measured.

- For the "pipe" cases, apart from the RNG model with the coarse mesh, the rest predicted within the MEV +/- STD lines.

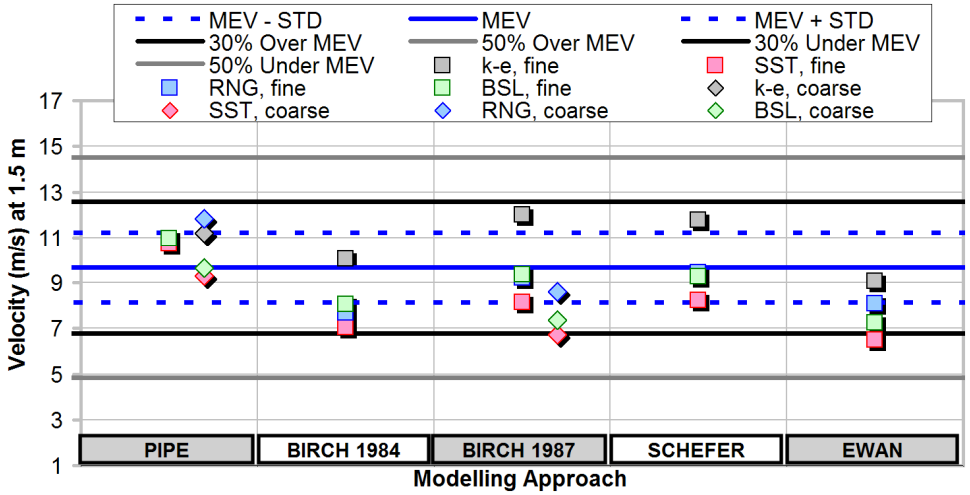


Figure 5. Axial velocity at 1.5 m from the release for all simulations considered

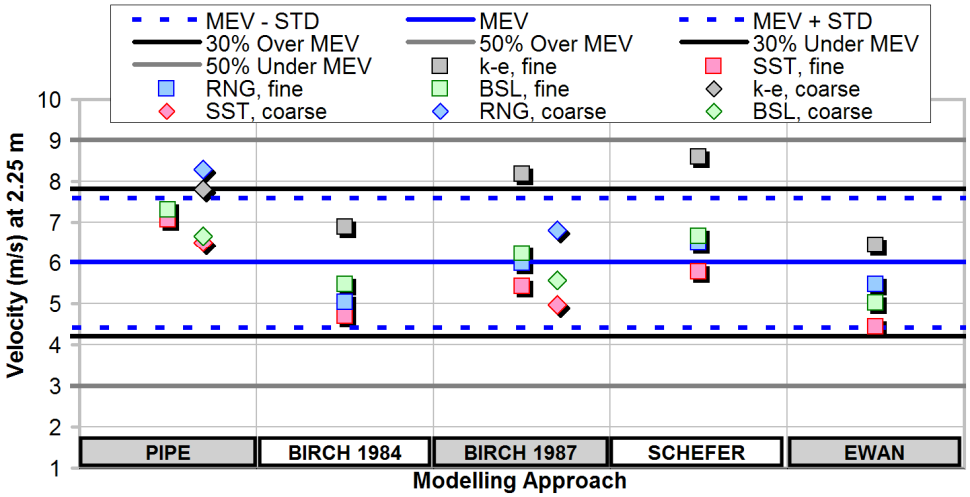


Figure 6. Axial velocity at 2.25 m from the release for all simulations considered

## 6.0 CONCLUSIONS

Performing simulations of under-expanded jets by resolving the jet's shock region is computationally quite expensive. To overcome such demands, several approaches have been proposed to model the source of the under-expanded jet within reasonable for engineering purposes computer run-times. This work presented an initial assessment of the predictions of four notional nozzle approaches (Birch 1984, Birch 1987, Schefer and Ewan) in connection to four commonly used turbulence models: the standard k-$\varepsilon$ epsilon, the Shear Stress Transport (SST), the ReNormalization Group (RNG) k-$\varepsilon$ and the Baseline k-omega (BSL). The numerical results were compared to experimental data of the flow velocity and $H_2$ concentration along the centerline of a jet issuing from 1 mm diameter nozzle at 98.1 bars. For comparison reasons, it was decided to simulate the $H_2$ release from a pipe of 10D length having a diameter equal to the experimental without the use of any notional nozzle approach with two unresolved meshes.

The predictions of the $H_2$ % concentration as compared to the experimental showed that the initial momentum flux at the source affects considerably the spreading rate of $H_2$ concentration at the jet's centreline. The approaches with the higher initial momentum flux (Birch 1987 and Schefer) performed better than the Birch 1984 and Ewan.

On the other hand, the highest concentrations, irrespective of the approach used, were predicted by the k-$\varepsilon$ followed by the RNG, BSL and finally SST. Surprisingly, modeling the actual pipe and using a mesh as computationally expensive as roughly the average between the "coarse" and "fine" of the notional nozzle simulations, produced satisfactory results. All predictions, including the ones with the finer mesh, were within the area of 30% Mean Experimental Value (MEV) over/under-prediction.

As expected, the higher axial velocities at 1.5 m and 2.25 m were predicted from the approaches with the higher release velocity arising from the momentum conservation assumption. Almost all of the results were located within the 30% of the MEV and none of them exceeded the 50% MEV over/under-prediction lines. Similarly to the $H_2$ concentration predictions, there is again a general tendency for higher predictions with k-$\varepsilon$, following by either RNG or BSL and lastly SST. For the "pipe" cases, apart from the RNG model with the coarse mesh, the rest predicted within the MEV +/- STD lines.

Numerical simulations of the release from the real pipe (without any notional diameter approach) were also carried out. The results of the simulations were in good agreement with the experimental data of the concentration field at 1.5 m and 2.25 m.

It must be emphasized that the conclusions of this analysis are specific to the experimental conditions, the numerical scheme and the computational mesh selected.

It is the intention of the authors to assess the approaches introduced here (and possibly the ones that assume the conservation of energy) to wider experimental conditions and to both axial and radial data measurements in order to draw general conclusions on the accuracy of the different notional nozzle approaches.

## 7.0 ACKNOWLEDGMENTS

The authors would like to thank Dr. Heitsch M. for his valuable comments on the paper and Dr. M. Kuznetsov for kindly providing the experimental data.

## 8.0 REFERENCES


1. Xu, B.P., Zhang, J.P., Wen, J.X., Dembele S. and Karwatzki J., "Numerical study of a highly under-expanded $H_2$ jet", 1st International Conference on Hydrogen Safety, 8-10 Sept. 2005, Pisa, Italy.
2. HYPER, "Releases, Fires and Explosions: Final Modelling Report", 2008.
3. Venetsanos, A.G., Papanikolaou, E. and Bartzis, J.G., The ADREA-HF CFD code for consequence assessment of hydrogen applications, *International Journal of Hydrogen Energy*, **35**, 2010, pp. 3908-39182.
4. Birch, A.D., Brown, D.R., Dodson, M.G. and Swaffield F., The structure and concentration decay of high pressure jets of natural gas, *Combustion Science and Technology*, **36**, 1984, pp. 249-261.
5. Venetsanos, A.G., Papanikolaou, E., Hansen, O.R., Middha, P., Garcia, J., Heitsch, M., Baraldi, D. and Adams P., HySafe standard benchmark problem SBEP-V11: Predictions of hydrogen release and dispersion from a CGH2 bus in an underpass, *International Journal of Hydrogen Energy*, **35**, 2010, pp. 3857-3867.
6. Venetsanos, A.G., Baraldi, D., Adams, P., Heggem, P.S. and Wilkening H., CFD modeling of hydrogen release, dispersion and combustion for automotive scenarios, *Journal of Loss Prevention in the Process Industries*, **21**, 2008, pp. 162-184.
7. Ivings, M.J., Gant, S.E., Saunders, C.J. and Pocock, D.J., Flammable gas cloud build up in a ventilated enclosure, *Journal of Hazardous Material*, **184**, 2010, pp. 170-176.
8. Brennan, S.L., Makarov, D.V., Molkov, V., LES of high pressure hydrogen jet fire, *Journal of Loss Prevention in the Process Industries*, **22**, 2009, pp. 353-359.
9. Hourri, A., Angers, B., Bénard, P., Surface effects on flammable extent of hydrogen and methane jets, *International Journal of Hydrogen Energy*, **34**, 2009, pp. 1569-1577.
10. Schefer, R.W., Houff, W.G., Williams, T.C., Bourne, B. and Colton, J., Characterization of high-pressure, underexpanded hydrogen-jet flames, *International Journal of Hydrogen Energy*, **32**, 2007, pp. 2081-2093.
11. Tchouvelev, A., Hydrogen Implementing Agreement, Task 19 – Hydrogen Safet, Knowledge gaps in hydrogen safety – A white paper, January 2008.
12. Baraldi, D., Papanikolaou, E., Heitsch, M., Moretto, P., Cant, S., Roekaerts, D., Dorofeev, S., Kotchourko, A., Middha, P., Tchouvelev, A., Ledin, S., Wen, J., Venetsanos, A., Molkov, V., Gap analysis of CFD modelling of accidental hydrogen release and combustion, JRC, Institute for Energy, The Netherlands, 2010, EUR 24399 EN.
13. HySafe, Biennal Report on Hydrogen Safetym Chapter III: Accidental phenomena and consequences, June 2007, http://www.hysafe.org/
14. Birch, A.D., Hughes, D.J. and Swaffield F., Velocity decay of high pressure jets, *Combustion Science and Technology*, **52**, 1987, pp. 161-171.
15. Ewan, B. C. R. and Moodie K., Structure and velocity measurements in underexpanded jets, *Combustion Science and Technology*, **45**, 1986, pp. 275-288.
16. Xiao, J., Travis, J.R. and Breitung, W., Hydrogen release from a high pressure gaseous hydrogen reservoir in case of a small leak", *International Journal of Hydrogen Energy*, **36**, 2011, pp. 2545-2554.
17. Yüceil, K.B. and Ötügen M. V., Scaling parameters for underexpanded supersonic jets, Physics of Fluids, **14**, 2002, pp. 4206-4215.
18. Molkov, V., Makarov, D., Bragin M., Physics and modelling of under-expanded jets and hydrogen dispersion in atmosphere, In: Physics of extreme state of matter 2009 (selected papers presented at the XXIII International Conference on Interaction of Intense Energy Fluxes with Matter, Elbrus, 1-6 March 2009), editors: Fortov V.E. et al., Chernogolovka, 143-145, 2009.
19. Kuznetsov, M., Grune, J., Veser, A., Friedrich, A., Kotchourko, N., Fast, G. and Jordan, T., Optical Observation and flame propagation in turbulent hydrogen jets, Proceedings of the 14th International Symposium on Flow Visualization, 21-24 June 2010, EXCO Daegu, Korea.

20. Veser, A., Kuznetsov, M., Fast, G., Friedrich, A., Kotchourko, N., Stern, G., Schwall, M. And Breitung, W., The structure and flame propagation regimes in turbulent hydrogen jets, *International Journal of Hydrogen Energy*, **36**, 2011, pp. 2351-2359.
21. ANSYS CFX-Solver Theory Guide, Release 12.0, April 2009
22. CFX-12.0, Documentation, Southpointe, 275 Technology Drive, Canonsburg, PA 15317, USA: ANSYS Inc., http://www.ansys.com
23. Tandra, D.S. et al, Numerical simulation of supersonic jet flow using a modified k-e model, *International Journal of Computational Fluid Dynamics*, **20**, 2006, pp. 19-27
24. D.C. Wilcox, Turbulence Modeling for CFD, 1994, DCW Industries, Inc., La Canada, California, 2nd printing